

Estradiol treatment increases M2-like visceral adipose tissue macrophages in obese ovariectomized mice regardless of its anorectic action

Kyeong-dae Kim^{a†}, Jeong Min Choe^{b†}, Soomin Myoung^b, Seung Hyun Lee^a, Minkyu Kim^a, Jae-Hoon Choi^a and Hyun Tae Park^b

^aDepartment of Life Science, College of Natural Sciences, Research Institute for Natural Sciences, Hanyang Institute of Bioscience and Biotechnology, Hanyang University, Seoul, Republic of Korea; ^bDepartment of Obstetrics and Gynecology, College of Medicine, Korea University, Seoul, Republic of Korea

ABSTRACT

Estradiol (E2) treatment has been known to induce changes in food intake, energy expenditure, and weight gain. However, its direct effects on adipose tissue macrophages (ATM) in vivo are not fully understood. Thus, we aimed to explore this aspect at cellular and molecular levels in ovariectomized obese mice. We examined the changes in ATMs after eight weeks of a high-fat diet (HFD) in male, female, and ovariectomized (OVX) mice. After eight weeks, osmotic pumps were inserted into OVX mice to provide two weeks of E2 treatment. We additionally set up a vehicle Pair-Fed (PF) control group that supplied the same amount of HFD consumed by the E2-treated group. We then investigated the in vivo phenotypic changes of visceral adipose tissue (VAT) macrophages. The percentage of M1-like ATMs decreased by the anorectic effect of E2, while M2-like ATMs increased regardless of the anorexia. E2 treatment increased the expression of anti-inflammatory genes but decreased pro-inflammatory genes in VAT. Monocyte recruitment and local proliferation contributed to M2-like ATMs. Furthermore, M2-like phenotypes were induced by E2 treatment in human macrophages. E2 treatment increases M2-like macrophages and improves the tissue milieu of VAT regardless of the anorectic reaction of E2.

ARTICLE HISTORY

Received 28 July 2022
Revised 16 September 2022
Accepted 21 September 2022
2022

KEYWORDS





Adipose tissue; appetite depressant; estradiol; macrophage; obesity

Introduction


Obesity is a global metabolic disease mainly caused by an imbalance between energy intake and expenditure. As obesity progresses, this energy overload pressures the adipose tissue environment, and low-grade and chronic inflammation occurs. This inflammatory state increases insulin resistance (IR) and type 2 diabetes risk (Xu et al. 2003; Hotamisligil 2006; Russo and Lumeng 2018). It is known that obesity-induced inflammation in adipose tissue causes an accumulation of immune cells, primarily pro-inflammatory macrophages (Hotamisligil et al. 1993; Ito et al. 2008). These macrophages differ from anti-inflammatory macrophages, which maintain adipose tissue homeostasis through anti-inflammatory mechanisms (Russo and Lumeng 2018). The accumulation of these adipose tissue macrophages (ATMs) affects adipose tissue inflammation and IR induction (Pekala et al. 1983; Hotamisligil et al. 1993; Parker et al. 2018). Although further studies are needed to

determine the exact mechanism of ATMs activation, there is evidence that adipocyte hypertrophy and local hypoxia caused by the energy imbalance results in their accumulation (Weisberg et al. 2003; Lumeng et al. 2007; Gericke et al. 2015). Another example of stimuli that activates ATMs is the crown-like structures (CLSs), a cluster produced by dead adipocytes surrounded by ATMs in obese adipose tissue (Cinti et al. 2005). Bone marrow-derived CD11c⁺ macrophages are the major class of recruited ATMs in CLSs, and CD11c⁺ cell removal attenuates obesity-induced inflammation and metabolic dysfunction (Patsouris et al. 2008).

The sex hormone, especially estrogen, is known to affect the adipose tissue environment and homeostasis. In humans, adipose tissue distribution is influenced by sex hormones (Regitz-Zagrosek et al. 2006; Jürimäe et al. 2010; Shi et al. 2013). In postmenopausal women, the accumulation of visceral adipose tissue (VAT) and the risk of cardiovascular disease increase due to

CONTACT Jae-Hoon Choi  jchoi75@hanyang.ac.kr  Department of Life Science, College of Natural Sciences, Research Institute of Natural Sciences, Hanyang Institute of Bioscience and Biotechnology, Hanyang University, Seoul 04763, Republic of Korea; Hyun Tae Park  cyberpelvis@gmail.com  Department of Obstetrics and Gynecology, Korea University College of Medicine, 73 Incheon-ro, Seongbuk-gu, Seoul 02841, Republic of Korea

[†]These authors contributed equally to this work

 Supplemental data for this article can be accessed at <https://doi.org/10.1080/19768354.2022.2128871>

© 2022 The Author(s). Published by Informa UK Limited, trading as Taylor & Francis Group

This is an Open Access article distributed under the terms of the Creative Commons Attribution-NonCommercial License (<http://creativecommons.org/licenses/by-nc/4.0/>), which permits unrestricted non-commercial use, distribution, and reproduction in any medium, provided the original work is properly cited.

decreased estrogen levels (Barton and Meyer 2009). These symptoms can be attenuated by treatment with 17 β -estradiol (E2), a type of estrogen produced mainly in the ovarian follicle (Barton and Meyer 2009; Christin-Maitre 2017). Additionally, E2 induces appetite suppression through a signalling pathway like leptin (Gao et al. 2007); this anorectic (appetite suppressant) reaction prevents excessive energy accumulation and obesity.

Collectively, obesity is not a simple metabolic disorder but a multifactorial disease with multiple components of the adipose tissue niche involved. E2 treatment has been known to attenuate VAT inflammation. This beneficial effect of E2 appears to be mediated in two mechanisms: anorectic and anti-inflammatory action. To dissect the effect of E2 treatment on VAT, we focused on the changes in ATMs by E2 treatment. In this study, we used a high-fat diet (HFD)-induced ovariectomized (OVX) mouse obesity model and performed E2 treatment via osmotic pump insertion. In addition, since the anorectic effect of E2 can affect ATMs, we performed pair-feeding in control and E2-treated mice to eliminate the anorectic effect of E2.

Materials and methods

Mice

C57BL/6 mice were purchased from Orient Bio (Sungnam, Republic of Korea). Whole-body GFP expressing mice (C57BL/6 background) were generously gifted from Dr. Goo Taeg Oh, Ewha Womans University, Republic of Korea. All mice were housed under specific pathogen-free conditions with a 12-hour light–dark cycle. Mice aged 7 weeks were fed with HFD (Rodent Diet with 60Kcal% Fat, cat. D12492; Research Diets Inc., New Brunswick, NJ, USA) to induce obesity. Female mice were sham-operated or OVX before inducing obesity. Obese OVX mice (OVX-HFD) were hypodermically implanted with an osmotic pump and administered E2 (3 μ g/day, cat. E8875; Sigma-Aldrich, St. Louis, MO, USA) for two weeks. All mice except for the vehicle pair-fed (PF) group had *ad libitum* (AL) access to HFD and water. The vehicle PF group was given the same amount of HFD that the E2-treated group consumed on average per day. All animal experiment protocols were approved by the Institutional Animal Care and Use Committee of the universities.

Antibodies and reagents

All sources of the antibodies and reagents are listed in the supplementary online table (Table S1).

Measurement of mouse body weight, energy intake, and E2 level

Mouse body weight and food intake (grams, g) were measured for each experiment. The total energy intake (kcal) was calculated from the consumed food (regular chow diet = 3.2 kcal/g, HFD = 5.24 kcal/g). Plasma samples were separated from mouse blood collected from the retro-orbital plexus, and E2 levels were examined using an enzyme-linked immunosorbent assay kit (cat. ab285237; Abcam, MA, USA). The body composition of vehicle PF and E2-treated mice was estimated using a mini-spec nuclear magnetic resonance spectrometer (cat. LF90; Bruker Corp., TX, USA).

Clodronate-loaded liposome injection to deplete blood monocytes

Clodronate-loaded liposomes were prepared as previously described (Amano et al. 2014). 200 μ l of clodronate-loaded liposomes was intravenously injected into the vehicle PF and E2-treated groups every 24 h. Every 12 h after the liposome injection, 100 μ l of 5-ethynyl-2'-deoxyuridine [EdU, 1 mg/ml in phosphate-buffered saline (PBS), cat. A10044; Molecular Probes, Eugene, OR, USA] was intraperitoneally administered to the mice. Flow cytometry assessed ATMs 84 h after the first liposome injection. 10 μ l of blood was taken before the liposome injections, and CD11b⁺ cells were analyzed to evaluate the blood monocytes using flow cytometry.

Bone marrow-derived monocyte injections

Bone marrow cells were isolated from the femur, tibia, and humerus of C57BL/6 GFP⁺ mice aged 8–9 weeks. To isolate pure monocytes, we used Miltenyi Biotec (Bergisch Gladbach, Germany) bone marrow isolation kit (cat. 130-100-629), LS columns (cat. 130-042-401), and VarioMACS separator (cat. 130-090-282) according to the manufacturer's instructions. The monocytes (2.0×10^6 cells) were suspended in 100 μ l PBS and injected into vehicle PF and E2-treated mice via the mouse tail vein after the osmotic pump was inserted.

VAT processing and flow cytometry analysis

VATs were excised from perigonadal white adipose tissue of all mice groups. The tissues were weighed and washed with PBS. Single cells from adipose tissue stromal vascular fractions (SVFs) were prepared as described earlier (Jang et al. 2020). The cells were analyzed using FACS CANTO II or FACS Fortessa flow

cytometer (BD Biosciences, Franklin Lakes, NJ) and FlowJo software (v9.8.0, Tree Star Inc., Ashland, OR, USA).

Immunostaining

VATs were fixed with 1% paraformaldehyde for 2 h and permeabilized for 30 min with 0.3% Triton X-100. Normal goat serum (5%) was used to block tissue for one hour at room temperature with gentle shaking. After blocking, the tissues were stained with primary antibodies (1:200) for 12 h at 4 °C and washed five times for ten minutes with a 0.3% Tween-20 detergent solution in PBS. The secondary antibodies (1:400) were stained for four hours and washed with PBS five times. VATs were stained with BODIPY for three minutes at room temperature in the dark to detect lipid droplets in the adipocytes. A confocal laser-scanning microscope (LSM 700; Carl Zeiss, Oberkochen, Germany) was used to observe the stained samples. The nucleus was stained with Hoechst 33342 (cat. 62249; Thermo Fisher Scientific, Waltham, MA, USA) or 4',6-diamidino-2-phenylindole (DAPI, cat. D1306; Invitrogen). The images were processed using the ImageJ software (1.49p, National Institutes of Health).

Human peripheral blood mononuclear cell (PBMC) culture

Human PBMCs were prepared as previously described (Luukkainen et al. 2018). Blood samples were collected from the subjects after obtaining written informed consent from the Declaration of Helsinki. 1×10^6 cells were plated in 24-well plates with complete media (RPMI 1640 with 10% heat-inactivated FBS, 1% L-glutamine, 1% penicillin–streptomycin, and 20 ng/ml macrophage colony-stimulating factor) and incubated for six days to differentiate into macrophages. The medium was changed every three days. From the 6th to 8th days, the media components were changed to RPMI 1640 supplemented with 10% charcoal-stripped FBS and 1% antibiotics. Simultaneously, E2 (0, 3, 10, and 30 nM) was added to the media, as indicated for each experiment.

Quantitative real-time polymerase chain reaction (qRT-PCR)

mRNA was extracted from 40 mg VAT using RNAiso Plus (cat. 9109; Takara Biotechnology Inc., Japan) and DNase I (cat. 18068-015; Invitrogen, Waltham, MA) according to the manufacturer's instructions. The RNA concentration was determined using a NanoDrop spectrophotometer

(TM ND-1000, NanoDrop Technologies Inc., Wilmington, DE), measuring absorbance at 260 and 280 nm. According to the manufacturer's instruction, cDNA was synthesized from 1 µg of total RNA using the PrimeScript RT–PCR kit (cat. RR-37A, Takara Biotechnology Inc., Japan). Real-time PCR was performed using the CFS96 Touch Real-Time System (Bio-Rad, USA). Each PCR sample mix contained 10 ng of cDNA, 1X SYBR green supermix (cat. 170-888, Bio-Rad, USA), and 0.5 µM of primer in a 20 µl reaction volume and then analyzed. The temperature profile was 95 °C for three minutes, amplification for 40 cycles: 30 s at 95 °C, 45 s at annealing temperatures for matching primers, and 30 s at 72 °C. The mRNA levels were normalized to the housekeeping gene *36b4* or *ACTB* using the $2^{-\Delta\Delta CT}$ method. The mouse and human primer sequences are listed in the supplementary online table (Table S2).

Statistical analysis

All results are shown as the mean \pm standard deviation or mean \pm standard error of the mean (qRT-PCR data). Before statistical analysis, we performed a normality test (Shapiro–Wilk) on the samples. A two-group independent t-test or one-way analysis of variance (ANOVA) with Bonferroni correction for post hoc multiple comparisons was used if the variables satisfied the normality assumption. Otherwise, the Mann–Whitney U test or Kruskal–Wallis ANOVA with Dunn's multiple comparison test was used. The statistical analysis was performed using GraphPad Prism 5 or InStat (GraphPad Software, La Jolla, CA, USA), with a *P*-value < 0.05 considered significant.

Results

Male and OVX-female mice are more susceptible to diet-induced obesity

To validate the obesity sensitivity of OVX mice, we first examined the body weight and VAT weight gains after 8 weeks of HFD (Figure 1A). Obese male and OVX mice continuously gained body weight during HFD, whereas the sham-operated female mice showed significant weight gain only after day 40 (Figure 1B). Previous studies revealed that OVX mice gain more weight than sham-operated mice (Rogers et al. 2009; Sul et al. 2021), and the OVX-chow mice gained more weight than female-chow mice even though they uptake similar calories (Figure 1B and S1A). After HFD, all obese mice gained more body and VAT weight than

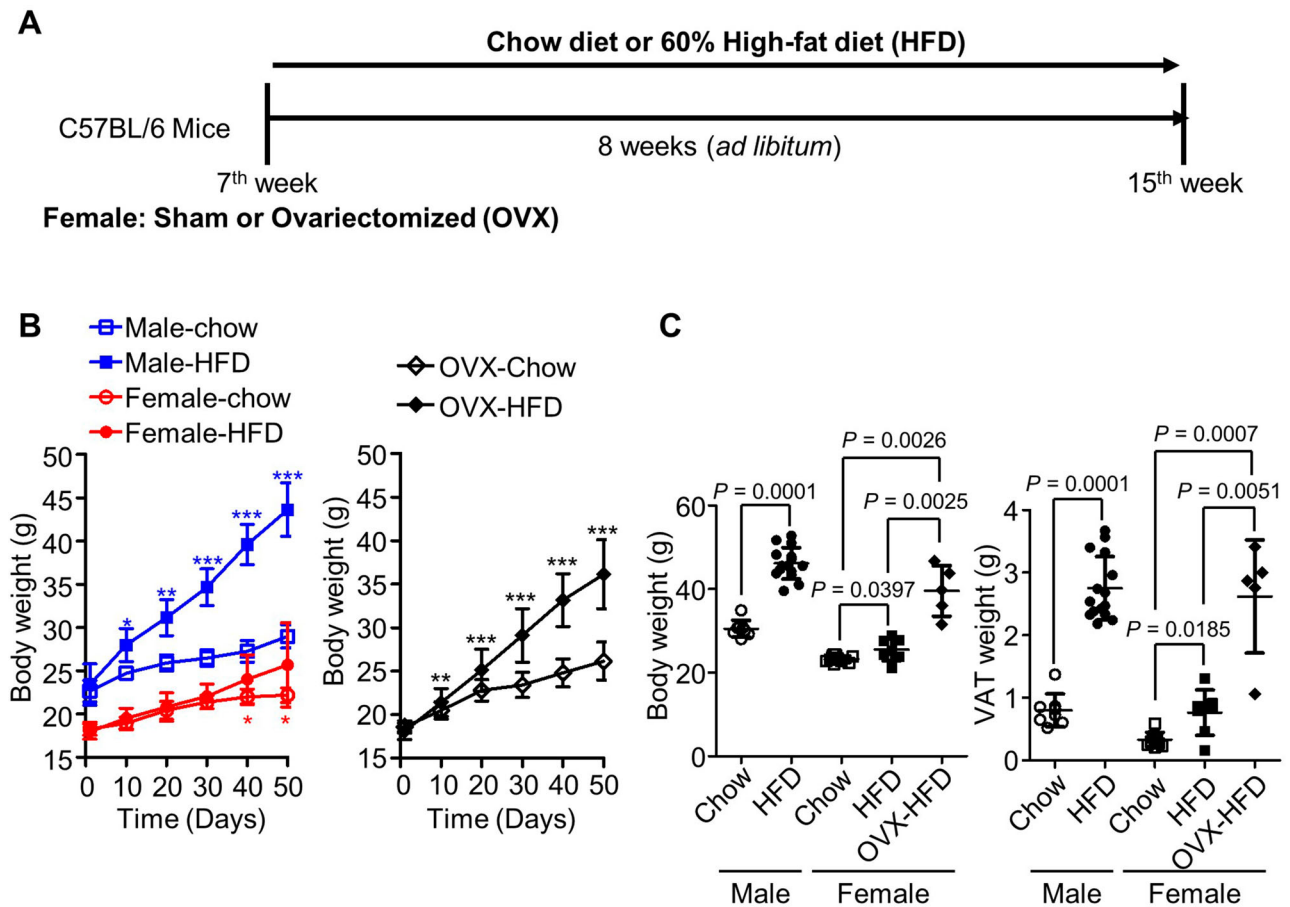


Figure 1. Body weight and visceral adipose tissue weight of a diet-induced obesity mouse model. (A) Experimental design for diet-induced obesity. (B) Changes in mouse body weight over 50 days. Stars indicate the P -values of the high-fat diet (HFD) group vs. control group for the day (male, $n = 8-10$, blue stars; sham-operated female, $n = 10-13$, red stars; ovariectomized female, $n = 47-49$, black stars). * $P < 0.05$, ** $P < 0.01$, *** $P < 0.001$. Non-significant P -values ($P \geq 0.05$) are not displayed in this graph. (C) Mouse body weight (left) and visceral adipose tissue (VAT) weight (right) after an 8-week chow diet or HFD. OVX, ovariectomized.

lean mice, and the OVX-HFD group even exhibited more weight gains than the sham-operated HFD group (Figure 1C). In addition, the VAT of the OVX-HFD group showed more CLSs – the hallmark of adipose tissue inflammation and accumulated a higher number of F4/80⁺ cells (murine macrophages) than the sham-operated HFD group (Figure S1B). These results suggest that female mice are more resistant to obesity than male mice, and estrogen depletion via ovariectomy makes them less resistant to obesity.

Male and OVX-female mice have more ATM accumulation during HFD

Using flow cytometry analysis, we examined VAT macrophages in obese mice. After extracting SVFs from VAT, we identified CD11b⁺CD64⁺ macrophages from CD45⁺ leukocytes (Figure 2A). We used two protein markers to show ATM subsets: CD11c and CD206 (macrophage mannose receptor), representing

pro-inflammatory M1-like ATMs and anti-inflammatory M2-like ATMs, respectively (Figure 2B). The obese male and OVX groups increased ATMs, especially M1-like ATMs, compared to their chow diet group and the OVX-HFD group also showed more CD11c⁺ macrophages than the sham-operated HFD group (Figure 2C and S2A). In contrast, the M2-like ATMs decreased in the male HFD and OVX-HFD group (Figure 2B and S2A), but there were no significant changes in the percentage of M2-like ATMs in SVFs (Figure 2C, right). These results suggest endogenous estrogen loss is related to pro-inflammatory macrophage accumulation into the VAT during obesity.

E2 treatment decreases the VAT adiposity compared to the pair-fed control OVX mice

We next examined the changes in obese OVX mice with E2 treatment. For this purpose, we subcutaneously inserted osmotic pumps into OVX-HFD mice and

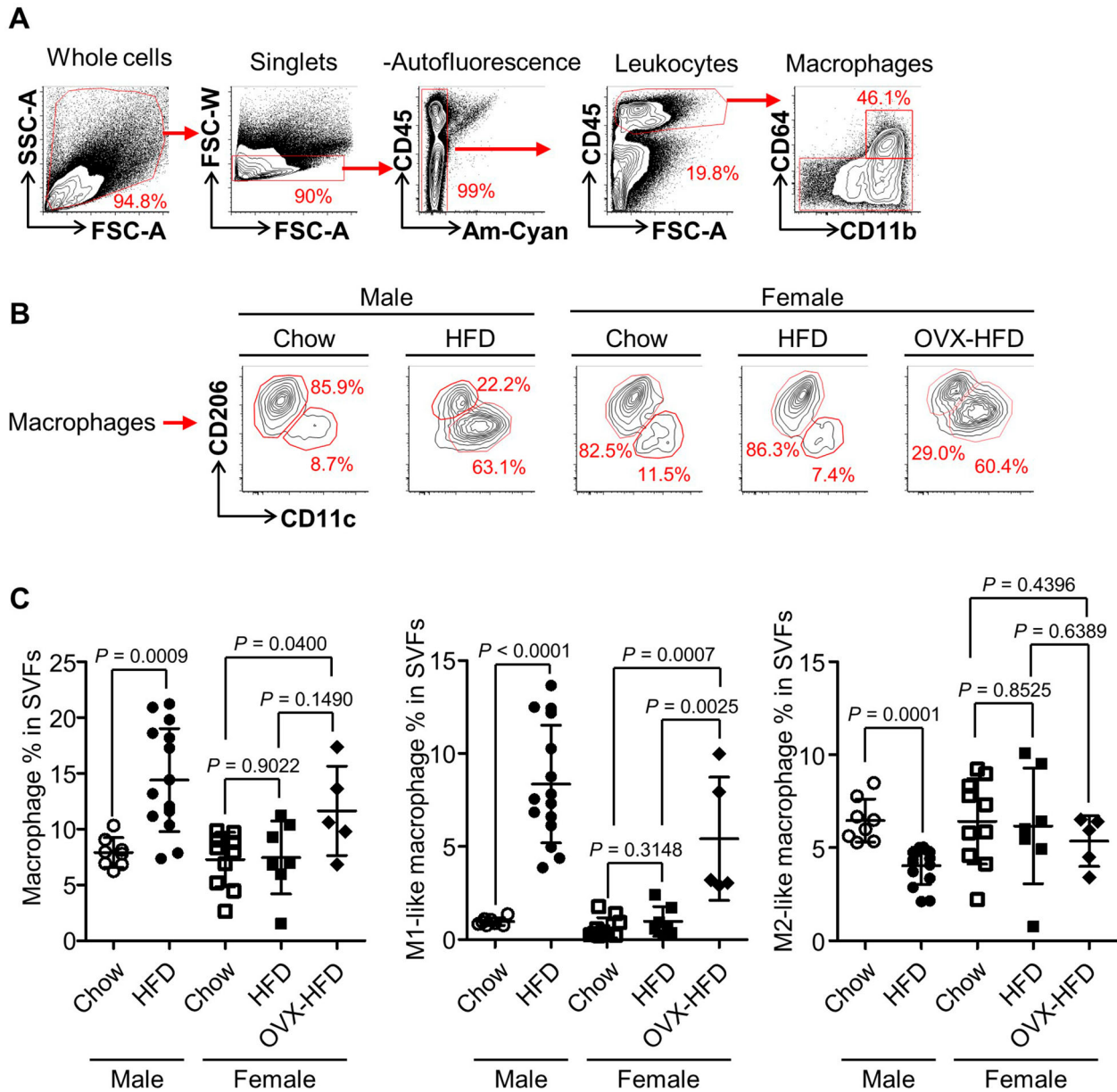


Figure 2. Analysis of the visceral adipose tissue macrophages (ATMs) using flow cytometry. The gating strategy (A) and representative plots of ATM subsets (B) of flow cytometric analysis. (C) Percentage of ATMs in stromal vascular fractions (SVFs). FSC, forward scatter; HFD, high-fat diet; OVX-HFD, high-fat diet fed-ovariectomized mice; SSC, side scatter.

continuously supplied E2 for two weeks (Figure 3A and S2B). During 8-week-HFD, the OVX mice took more calories than their control group (Figure S1A). However, during E2 treatment, the E2-treated OVX group showed significantly lower calorie intake and weight gain than the control vehicle AL group (Figure 3(B and C)). Since dietary control is one of the essential factors in improving obesity, we set up a vehicle PF control group to eliminate the anorectic effect of E2 treatment (Figure 3(A and B)).

The E2-treated group decreased body weight compared with the vehicle AL group, but did not change

when compared with the vehicle PF group (Figure 3C and D, left). However, VAT weight decreased in the E2-treated group compared to both vehicle groups (Figure 3D, right). Nuclear magnetic resonance (NMR) analysis also showed a significantly reduced fat composition in the E2-treated group compared to the vehicle PF group (Figure 3E). These results suggest two aspects of the E2 treatment on obese OVX mice. First, the anorectic reaction of E2 significantly impacts the body- and VAT-weight in obesity. Second, regardless of this anorexia, E2 treatment directly reduces VAT adiposity in OVX mice.

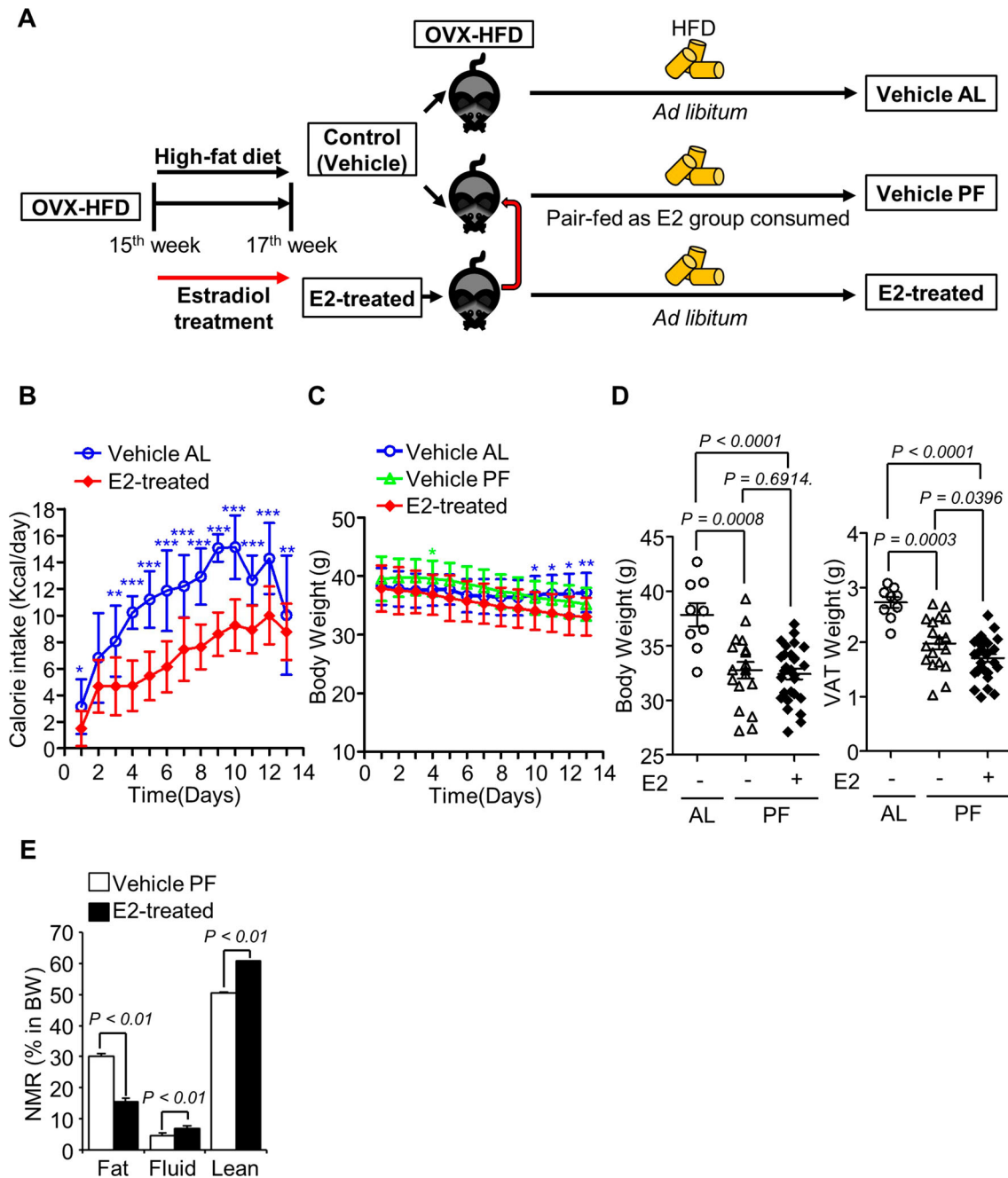


Figure 3. Estradiol (E2) treatment induces body weight and visceral adipose tissue changes in obese ovariectomized (OVX-HFD) mice. (A) Experimental design for E2 treatment. (B and C) Daily calorie intake (B) and body weight (C) during E2 treatment. Stars indicate *P*-values compared vehicle AL with E2-treated group (blue stars, $n = 8-22$) or vehicle PF and E2-treated group (green stars, $n = 8-22$). * $P < 0.05$, ** $P < 0.01$. Non-significant *P*-values ($P \geq 0.05$) are not displayed in this graph. (D) Body weight (left) and visceral adipose tissue weight (VAT, Right) after E2 treatment. (E) Nuclear Magnetic Resonance (NMR) analysis of Mouse body composition. AL, *ad libitum*; BW, body weight; PF, pair-fed.

E2 treatment increases M2-like macrophages in VAT compared to the pair-fed control OVX mice

To investigate ATM accumulation after E2 treatment, we performed the flow cytometry analysis. The E2 treatment did not show any overall changes in VAT macrophages compared with the vehicle AL group (Figure 4(A and B)). However, the reduced calorie uptake (vehicle AL

vs. vehicle PF) decreased ATM accumulation. When comparing the vehicle PF with the E2-treated group, ATMs increased in the E2-treated group. This change in ATM populations was confirmed in the ATM subset (Figure 4(A and C)). M1-like macrophages decreased between the vehicle AL and vehicle PF groups but did not decrease between the vehicle PF and E2 groups

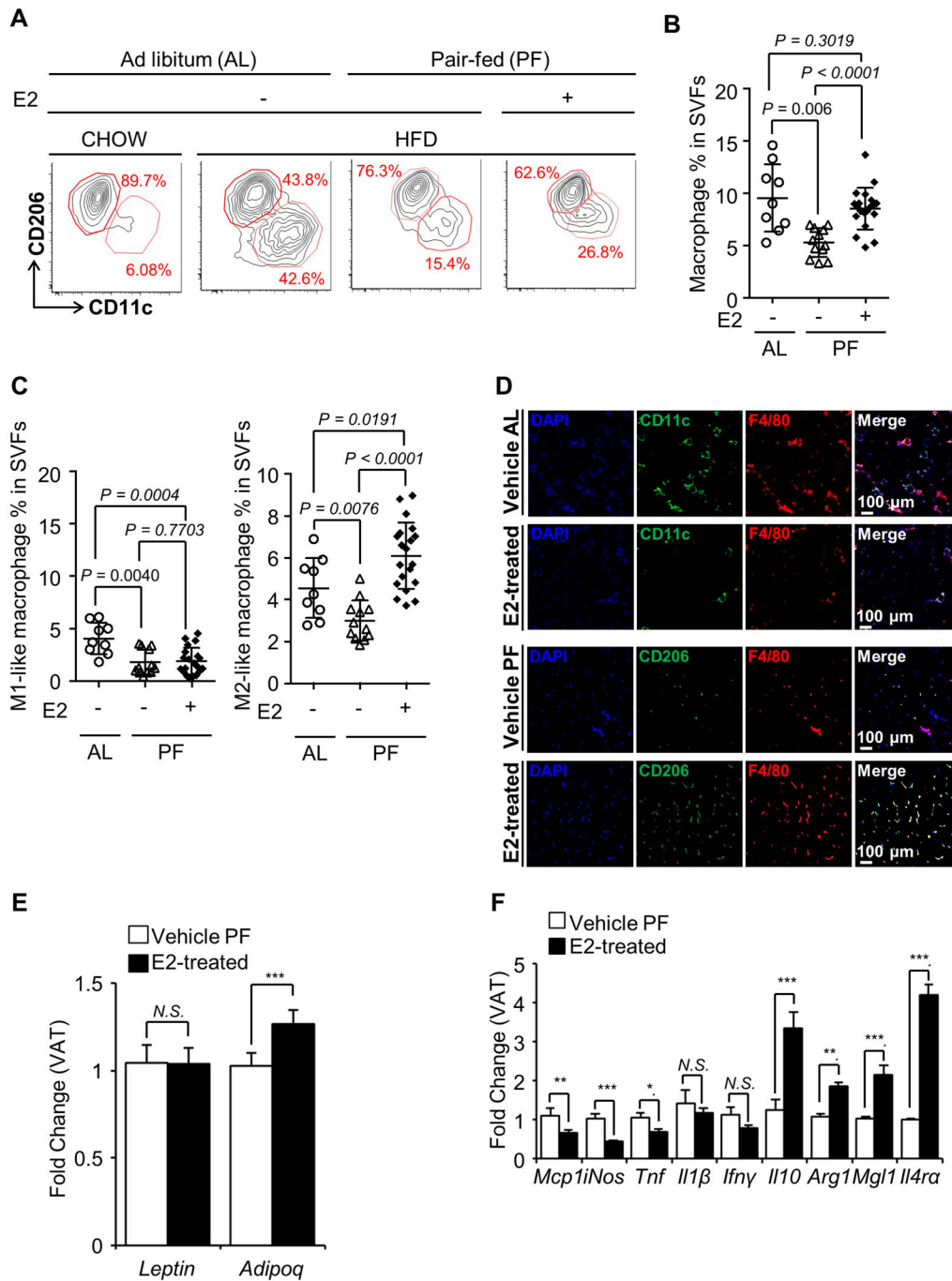


Figure 4. Change of the macrophage subsets and visceral adipose tissue (VAT) milieu after two weeks of estradiol (E2) treatment. (A) Representative plots of VAT macrophages on vehicle *ad libitum* (AL), vehicle pair-fed (PF), and E2-treated groups. (B and C) Percentage of VAT macrophages (B) and their subsets (C) ($n = 9\text{--}20$). (D) Visualization of CD11c, CD206 and F4/80 VAT ($n = 3$). VAT mRNA expression levels of adipokines (E) and pro-inflammatory or anti-inflammatory genes (F), (base = 1, $n = 3\text{--}12$). * $P < 0.05$, ** $P < 0.01$, *** $P < 0.001$, N.S., non-significant. SVFs, stromal vascular fractions.

(Figure 4C, left). M2-like macrophages decreased in the vehicle PF group compared with the vehicle AL group but significantly increased in the E2 group compared with the vehicle AL or vehicle PF groups (Figure 4C, right). These results indicate that the composition of ATM populations resulting from the E2 treatment (vehicle AL vs. E2) is not a unilateral decrease or increase

in the pro- or anti-inflammatory macrophages, respectively. These results also suggest that M1-like ATMs may decrease by the appetite-inhibiting effect of E2 (vehicle AL vs. vehicle PF). Regardless of the anorectic consequences, the estrogen treatment increases the M2-like macrophage levels compared to M1-like macrophage levels (vehicle PF vs. E2).

This phenomenon was also confirmed by immunostaining of VAT (Figure 4D). The CD11c⁺ and F4/80⁺ cells, which indicate inflammatory macrophages in VAT CLSs (Figure S1B), significantly decreased in the E2-treated group compared with the vehicle AL group (Figure 4D, top). On the other hand, E2-treated mice showed more F4/80⁺ and CD206⁺ VAT cells than the vehicle PF group (Figure 4D, bottom). Next, we examined the expression level of two adipokines: *Leptin* and *Adipoq* (encoding adiponectin). Between them, only *Adipoq* showed a significant increase in the E2-treated group, compared to the vehicle PF group (Figure 4E). Adiponectin is known to promote M2-like ATM polarization (Ohashi et al. 2010). Therefore, we compared the vehicle PF and E2 groups to confirm changes in the VAT environment through qPCR analysis. Inflammatory genes, such as *Mcp-1*, *iNos*, and *Tnf* decreased, whereas

anti-inflammatory genes *Il-10*, *Arg1*, *Mgl1*, and *Il-4ra* increased in the E2-treated group compared with the vehicle PF group (Figure 4F). This result suggests that E2 treatment induces an anti-inflammatory adipose tissue milieu by increasing M2-like ATMs and anti-inflammatory genes regardless of the anorectic effect.

Monocyte recruitment and local proliferation are responsible for increasing M2-like ATMs by E2 treatment

To understand the source of the increased M2-like ATMs, we examined the M2-like ATM proliferation in the E2-treated group when an external influx of blood monocytes (CD11b⁺ cells) was suppressed by clodronate-liposome injection (Amano et al. 2014) (Figure 5A, left). The blood monocytes were

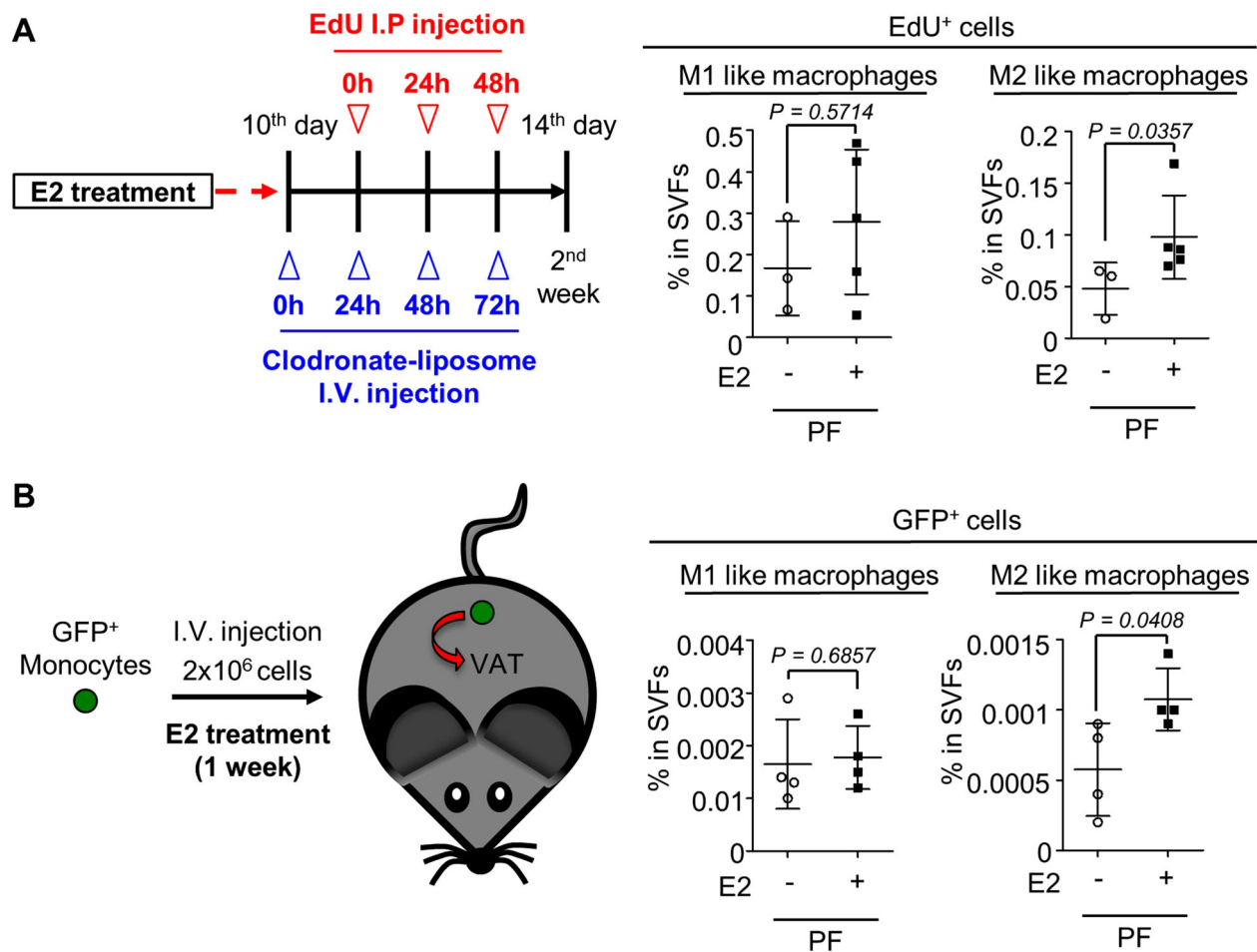


Figure 5. Estradiol (E2)-induced M2-like macrophages are related to macrophage proliferation and monocyte recruitment. (A) Left: the injection plan of Clodronate-liposome and 5-ethynyl-2'-deoxyuridine (EdU) for vehicle pair-fed (PF) and E2-treated mice. Right: percentages of EdU⁺ macrophages in stromal vascular fractions (SVFs) after administration of clodronate-liposome. (B) Left: Bone marrow-derived monocytes expressing green fluorescent protein (GFP) were injected into vehicle PF and E2-treated mice. Right: GFP⁺ macrophage percentages after one-week monocyte injection. I.P., intraperitoneal; I.V., intravenous; VAT, visceral adipose tissue.

significantly reduced by clodronate-liposome administration (Figure S3A). We injected 5-ethynyl-2'-deoxyuridine (EdU) to label the proliferating cells. We found that the EdU⁺ M2-like ATMs of the E2-treated group increased compared with vehicle PF despite the decrease in monocyte recruitment (Figure 5A, right), whereas M1-like ATM numbers showed no significant changes.

Next, we injected GFP⁺ bone marrow-derived monocytes into the mice and investigated the GFP-expressing cells in M2-like ATMs (Figure 5B, left). As a result, GFP⁺ M2-like ATMs increased in the E2 group (Figure 5B, right). These results suggest that E2 treatment influences

M2-like ATMs both from the blood-origin and local proliferation, and the regional expansion is the primary source of the macrophages.

E2 treatment induces M2-like cell polarization in human macrophages

We investigated whether the E2 action occurs in human macrophages using a human peripheral blood nucleus cell (PBMC) culture. We extracted human PBMCs and incubated cells (1×10^6) with M-CSF for six days and then treated culture media with E2 0–30 nM for 48 h (Figure 6A). The CD206 level was higher than that in the control

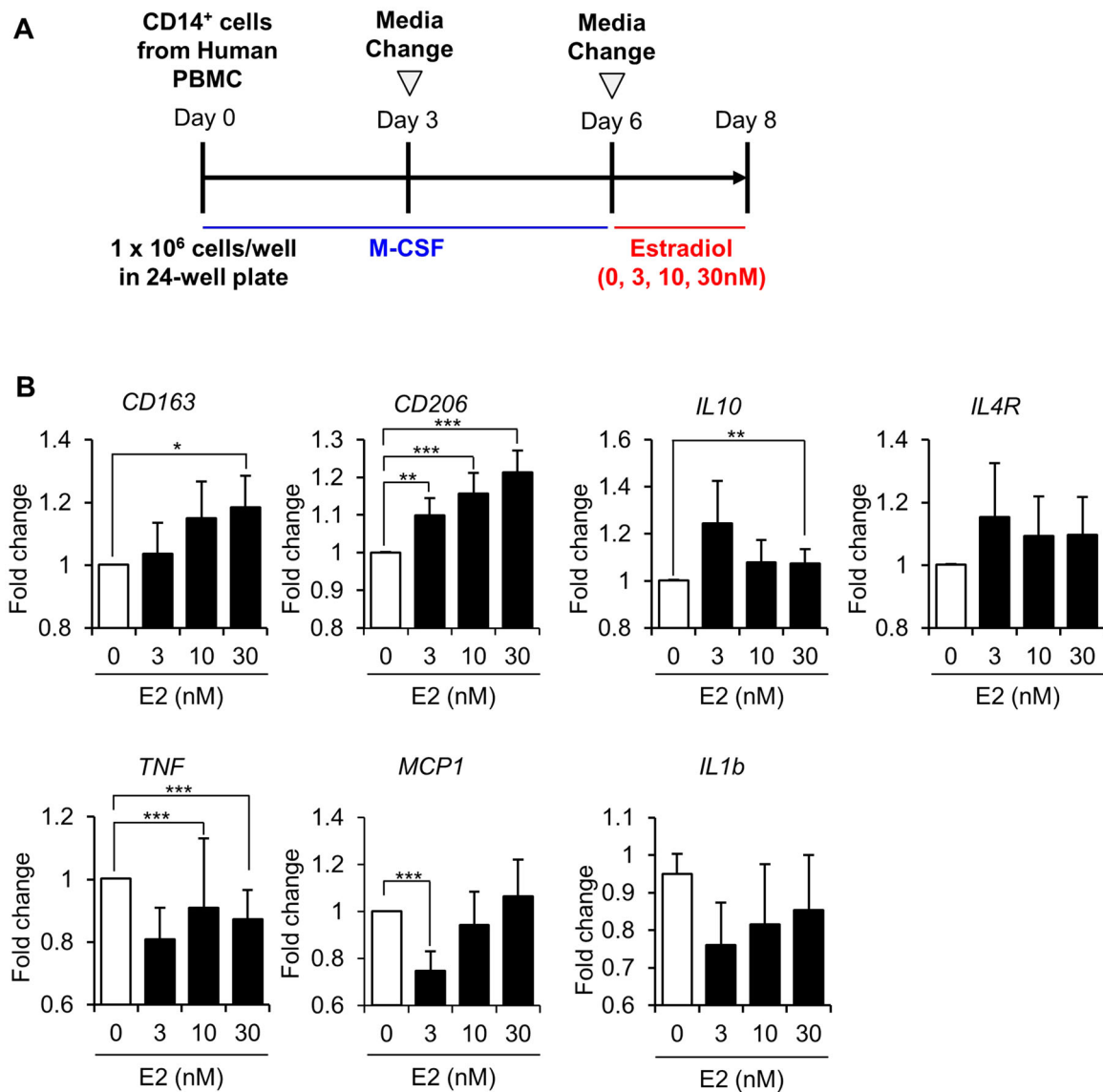


Figure 6. M2-like macrophage polarization via estradiol (E2) treatment in human CD14⁺ cell-derived macrophages. (A) Experimental design for E2-induced human macrophage polarization from peripheral blood mononuclear cells (PBMCs). (B) Comparison of mRNA expression of human macrophages ($n = 5-7$) treated with E2 for 48 h (concentration: 0, 3, 10, and 30 nM). The fold changes were compared to the untreated cells (base = 1). * $P < 0.05$, ** $P < 0.01$, *** $P < 0.001$. Non-significant P -values ($P \geq 0.05$) are not displayed in this graph. M-CSF, Macrophage colony-stimulating factor.

group for all E2 treatment concentrations, and *CD163* and *IL10* levels were significantly increased upon treatment with 30 nM of E2. *TNF* expression decreased at 10 and 30 nM E2 concentrations, while *MCP1* levels decreased only after 3 nM of E2 treatment. *IL4R* and *IL1B* levels showed no significant differences after E2 treatment (Figure 6B). Altogether, E2 treatment increases expression of alternative macrophage genes such as *CD163*, *CD206*, and *IL10* in human PBMC-derived macrophages.

Discussion

Since obesity occurs due to the energy imbalance caused by excessive nutrition (Hotamisligil 2006), we should consider the effects of this energy accumulation when studying this metabolic disorder. In the case of estrogen, the hormone suppresses appetite by a similar pathway as leptin (Gao et al. 2007). Therefore, to determine *in vivo* E2 effect on obesity, the variables should be considered according to this anorectic effect.

As expected, our E2-treated mice consumed less HFD than the control mice (vehicle AL vs. E2 group, Figure 3B). The decrease of body weight and M1-like ATMs (Figure 3C and Figure 4C) was related to the calorie uptake reduction (vehicle AL vs. PF group). To compensate for this calorie intake inhibitory effect, we set up a vehicle PF control group that received the same amount of feed consumed by the E2-treated group. By comparing Vehicle PF and E2-treated groups, we excluded the anorectic effect of E2 and solely confirmed the impact of the E2 treatment on the VAT and M2-like macrophages (Figure 3D, Figure 4C–F). In addition to our ATM study, a recent report showed that regulatory T cells increased during long-term HFD and E2 treatment (Ishikawa et al. 2020). The ATMs and regulatory T cells are crucial immune cells in VAT homeostasis. Further, research for other adipose tissue immune cells is also required.

Our study did not focus on a molecular pathway of the M2-like macrophage increase due to E2 treatment, but the increased macrophage population is consistent with the previous studies (Pepe et al. 2017; Sul et al. 2021). E2 treatment to peritoneal macrophages increases gene expressions related to cell proliferation, anti-inflammatory responses, and wound healing (Pepe et al. 2017). A recent study revealed that increased heme oxygenase-1 expression with E2 treatment polarized the M2-like macrophage population (Sul et al. 2021). The induced heme oxygenase-1 lowered macrophage reactive oxygen species levels, enhancing M2 polarization.

Furthermore, we found that the increased M2-like ATMs are from local proliferation and monocyte

recruitment (Figure 5(A and B)). We also confirmed gene expression patterns of E2 treated-human cultured macrophages. Although human macrophages show a mixture of phenotypes of M1-like and M2-like macrophages (Zeyda et al. 2007; Bourlier et al. 2008; Wentworth et al. 2010; Hill et al. 2018), the cultured human PBMC-derived macrophages showed anti-inflammatory gene expressions after E2 treatment. The result suggests an alternative activation of human macrophages (Figure 6B) is similar to our mouse model and reported result (Toniolo et al. 2015).

In conclusion, we confirmed that the E2 treatment showed anti-inflammatory effects on the adipose tissue environment and ATMs, even excluding the energy intake inhibitory effect. Hence, our results suggest that E2 therapy could directly alleviate obesity-induced adipose tissue inflammation in postmenopausal women.

Disclosure statement

No potential conflict of interest was reported by the author(s).

Funding

This work was supported by National Research Foundation of Korea: [Grant Number 2021R1A2C3004586 and 2016M3A9D5A01952413] and Ministry of Health and Welfare (MOHW, Korea): [Grant Number HI21C1560].

References

- Amano SU, Cohen JL, Vangala P, Tencerova M, Nicoloso SM, Yawe JC, Shen Y, Czech MP, Aouadi M. 2014. Local proliferation of macrophages contributes to obesity-associated adipose tissue inflammation. *Cell Metab.* 19(1):162–171.
- Barton M, Meyer MR. 2009. Postmenopausal hypertension: mechanisms and therapy. *Hypertension.* 54(1):11–18.
- Bourlier V, Zakaroff-Girard A, Miranville A, De Barros S, Maumus M, Sengenès C, Galitzky J, Lafontan M, Karpe F, Frayn KN, et al. 2008. Remodeling phenotype of human subcutaneous adipose tissue macrophages. *Circulation.* 117(6):806–815.
- Christin-Maitre S. 2017. Use of hormone replacement in females with endocrine disorders. *Horm Res Paediatr.* 87(4):215–223. eng.
- Cinti S, Mitchell G, Barbatelli G, Murano I, Ceresi E, Faloia E, Wang S, Fortier M, Greenberg AS, Obin MS. 2005. Adipocyte death defines macrophage localization and function in adipose tissue of obese mice and humans. *J Lipid Res.* 46(11):2347–2355.
- Gao Q, Mezei G, Nie Y, Rao Y, Choi CS, Bechmann I, Leranth C, Toran-Allerand D, Priest CA, Roberts JL, et al. 2007. Anorectic estrogen mimics leptin's effect on the rewiring of melanocortin cells and Stat3 signaling in obese animals. *Nat Med.* 13(1):89–94.
- Gericke M, Weyer U, Braune J, Bechmann I, Eilers J. 2015. A method for long-term live imaging of tissue macrophages

- in adipose tissue explants. *Am J Physiol - Endocrinol Metab.* 308(11):E1023–E1033.
- Hill DA, Lim HW, Kim YH, Ho WY, Foong YH, Nelson VL, Nguyen HCB, Chegireddy K, Kim J, Habertheuer A, et al. 2018. Distinct macrophage populations direct inflammatory versus physiological changes in adipose tissue. *Proc Natl Acad Sci U S A.* 115(22):E5096–E5105.
- Hotamisligil GS. 2006. Inflammation and metabolic disorders. *Nature.* 444(7121):860–867. eng.
- Hotamisligil GS, Shargill NS, Spiegelman BM. 1993. Adipose expression of tumor necrosis factor- α : direct role in obesity-linked insulin resistance. *Science.* 259(5091):87–91.
- Ishikawa A, Wada T, Nishimura S, Ito T, Okekawa A, Onogi Y, Watanabe E, Sameshima A, Tanaka T, Tsuneki H, et al. 2020. Estrogen regulates sex-specific localization of regulatory T cells in adipose tissue of obese female mice. *PLoS One.* 15(4):e0230885.
- Ito A, Suganami T, Yamauchi A, Degawa-Yamauchi M, Tanaka M, Kouyama R, Kobayashi Y, Nitta N, Yasuda K, Hirata Y, et al. 2008. Role of CC chemokine receptor 2 in bone marrow cells in the recruitment of macrophages into obese adipose tissue. *J Biol Chem.* 283(51):35715–35723.
- Jang HS, Kim K, Lee MR, Kim SH, Choi JH, Park MJ. 2020. Treatment of growth hormone attenuates hepatic steatosis in hyperlipidemic mice via downregulation of hepatic CD36 expression. *Animal Cells Syst (Seoul).* 24(3):151–159.
- Jürimäe J, Hills AP, Jürimäe T. 2010. Cytokines, growth mediators, and physical activity in children during puberty. Basel: Karger. (Medicine and sport science,; 55).
- Lumeng CN, Deyoung SM, Bodzin JL, Saltiel AR. 2007. Increased inflammatory properties of adipose tissue macrophages recruited during diet-induced obesity. *Diabetes.* 56(1):16–23.
- Luukkainen A, Puan KJ, Yusof N, Lee B, Tan KS, Liu J, Yan Y, Toppila-Salmi S, Renkonen R, Chow VT, et al. 2018. A coculture model of PBMC and stem cell derived human nasal epithelium reveals rapid activation of NK and innate T cells upon influenza A virus infection of the nasal epithelium. *Front Immunol.* 9:2514.
- Ohashi K, Parker JL, Ouchi N, Higuchi A, Vita JA, Gokce N, Pedersen AA, Kalthoff C, Tullin S, Sams A, et al. 2010. Adiponectin promotes macrophage polarization toward an anti-inflammatory phenotype. *J Biol Chem.* 285(9):6153–6160.
- Parker R, Weston CJ, Miao Z, Corbett C, Armstrong MJ, Ertl L, Ebsworth K, Walters MJ, Baumart T, Newland D, et al. 2018. CC chemokine receptor 2 promotes recruitment of myeloid cells associated with insulin resistance in nonalcoholic fatty liver disease. *Am J Physiol-Gastrointest Liver Physiol.* 314(4):G483–G493.
- Patsouris D, Li PP, Thapar D, Chapman J, Olefsky JM, Neels JG. 2008. Ablation of CD11c-positive cells normalizes insulin sensitivity in obese insulin resistant animals. *Cell Metab.* 8(4):301–309.
- Pekala P, Kawakami M, Vine W, Lane MD, Cerami A. 1983. Studies of insulin resistance in adipocytes induced by macrophage mediator. *J Exp Med.* 157(4):1360–1365.
- Pepe G, Braga D, Renzi TA, Villa A, Bolego C, D'Avila F, Barlassina C, Maggi A, Locati M, Vegeto E. 2017. Self-renewal and phenotypic conversion are the main physiological responses of macrophages to the endogenous estrogen surge. *Sci Rep.* 7:44270.
- Regitz-Zagrosek V, Lehmkuhl E, Weickert MO. 2006. Gender differences in the metabolic syndrome and their role for cardiovascular disease. *Clin Res Cardiol.* 95(3):136–147.
- Rogers NH, Perfield JW, 2nd, Strissel KJ, Obin MS, Greenberg AS. 2009. Reduced energy expenditure and increased inflammation are early events in the development of ovariectomy-induced obesity. *Endocrinology.* 150(5):2161–2168.
- Russo L, Lumeng CN. 2018. Properties and functions of adipose tissue macrophages in obesity. *Immunology.* 155(4):407–417. eng.
- Shi H, Kumar SP, Liu X. 2013. G protein-coupled estrogen receptor in energy homeostasis and obesity pathogenesis. *Prog Mol Biol Transl Sci.* 114:193–250.
- Sul OJ, Hyun HJ, Rajasekaran M, Suh JH, Choi HS. 2021. Estrogen enhances browning in adipose tissue by M2 macrophage polarization via heme oxygenase-1. *J Cell Physiol.* 236(3):1875–1888.
- Toniolo A, Fadini GP, Tedesco S, Cappellari R, Vegeto E, Maggi A, Avogaro A, Bolego C, Cignarella A. 2015. Alternative activation of human macrophages is rescued by estrogen treatment in vitro and impaired by menopausal status. *J Clin Endocrinol Metab.* 100(1):E50–E58.
- Weisberg SP, McCann D, Desai M, Rosenbaum M, Leibel RL, Ferrante AW, Jr. 2003. Obesity is associated with macrophage accumulation in adipose tissue. *J Clin Invest.* 112(12):1796–1808.
- Wentworth JM, Naselli G, Brown WA, Doyle L, Phipson B, Smyth GK, Wabitsch M, O'Brien PE, Harrison LC. 2010. Pro-inflammatory CD11c + CD206 + adipose tissue macrophages are associated with insulin resistance in human obesity. *Diabetes.* 59(7):1648–1656.
- Xu H, Barnes GT, Yang Q, Tan G, Yang D, Chou CJ, Sole J, Nichols A, Ross JS, Tartaglia LA, et al. 2003. Chronic inflammation in fat plays a crucial role in the development of obesity-related insulin resistance. *J Clin Invest.* 112(12):1821–1830. eng.
- Zeyda M, Farmer D, Todoric J, Aszmann O, Speiser M, Gyori G, Zlabinger GJ, Stulnig TM. 2007. Human adipose tissue macrophages are of an anti-inflammatory phenotype but capable of excessive pro-inflammatory mediator production. *Int J Obes.* 31(9):1420–1428.